

<sup>1</sup>

# How is experience transformed into memory?

<sup>2</sup> Andrew C. Heusser, Paxton C. Fitzpatrick, and Jeremy R. Manning

Department of Psychological and Brain Sciences

Dartmouth College, Hanover, NH 03755, USA

Corresponding author: jeremy.r.manning@dartmouth.edu

<sup>3</sup> September 7, 2018

<sup>4</sup> **Abstract**

<sup>5</sup> The ways our experiences unfold over time define unique *trajectories* through the relevant  
<sup>6</sup> representational spaces. Within this geometric framework, one can compare the shape of the  
<sup>7</sup> trajectory formed by an experience to that defined by our later remembering of that experience.  
<sup>8</sup> We propose a framework for mapping naturalistic experiences onto geometric spaces that char-  
<sup>9</sup> acterize how they unfold over time. We apply this approach to a naturalistic memory experiment  
<sup>10</sup> which had participants view and recount a video. We found that the shapes of the trajectories  
<sup>11</sup> formed by participants' recounts were all highly similar to that of the original video, but par-  
<sup>12</sup> ticipants differed in the level of detail they remembered. We also identified a network of brain  
<sup>13</sup> structures that are sensitive to the "shapes" of our ongoing experiences, and an overlapping  
<sup>14</sup> network that is sensitive to how we will later remember those experiences.

<sup>15</sup>

## Introduction

<sup>16</sup> What does it mean to *remember* something? In traditional episodic memory experiments (e.g.,  
<sup>17</sup> list-learning or trial-based experiments; Murdock, 1962; Kahana, 1996), remembering is often cast  
<sup>18</sup> as a discrete and binary operation: each studied item may be separated from the rest of one's

19 experiences, and that item may be labeled as having been recalled versus forgotten. More nuanced  
20 studies might incorporate self-reported confidence measures as a proxy for memory strength, or  
21 ask participants to discriminate between “recollecting” the (contextual) details of an experience or  
22 having a general feeling of “familiarity” (Yonelinas, 2002). However, characterizing and evaluating  
23 memory in more realistic contexts (e.g., recounting a recent experience to a friend) is fundamentally  
24 different in at least three ways (for review also see Koriat and Goldsmith, 1994; Huk et al., 2018).  
25 First, real world recall is continuous, rather than discrete. Unlike in trial-based experiments,  
26 removing a (naturalistic) event from the context in which it occurs can substantially change its  
27 meaning. Second, the specific words used to describe an experience have little bearing on whether  
28 the experience should be considered to have been “remembered.” Asking whether the rememberer  
29 has precisely reproduced a specific set of words to describe a given experience is nearly orthogonal  
30 to whether they were actually able to remember it. In classic (e.g., list-learning) memory studies,  
31 by contrast, counting the number or proportion of precise recalls is often a primary metric of  
32 assessing the quality of participants’ memories. Third, one might remember the *gist* or essence  
33 of an experience but forget (or neglect to recount) particular details. Capturing the gist of what  
34 happened is typically the main “point” of recounting a memory to a listener whereas, depending  
35 on the circumstances, accurate recall of any specific detail may be irrelevant. There is no analog  
36 of the gist of an experience in most traditional memory experiments; rather we tend to assess  
37 participants’ abilities to recover specific details (e.g., computing the proportion of specific stimuli  
38 they remember, which presentation positions the remembered stimuli came from, etc.).

39 How might one go about formally characterizing the gist of an experience, or whether that gist  
40 has been recovered by the rememberer? Any given moment of an experience derives meaning from  
41 surrounding moments, as well as from longer-range temporal associations (e.g., Lerner et al., 2011).  
42 Therefore the timecourse describing how an event unfolds is fundamental to its overall meaning.  
43 Further, this hierarchy formed by our subjective experiences at different timescales defines a  
44 *context* for each new moment (e.g., Howard and Kahana, 2002; Howard et al., 2014), and plays an  
45 important role in how we interpret that moment and remember it later (for review see Manning  
et al., 2015). Our memory systems can then leverage these associations to form predictions that

47 help guide our behaviors (Ranganath and Ritchey, 2012). For example, as we navigate the world,  
48 the features of our subjective experiences tend to change gradually (e.g., the room or situation we  
49 are in is strongly temporally autocorrelated), allowing us to form stable estimates of our current  
50 situation and behave accordingly (Zacks et al., 2007; Zwaan and Radvansky, 1998). Although our  
51 experiences most often change gradually, they also occasionally change suddenly (e.g., when we  
52 walk through a doorway; Radvansky and Zacks, 2017). Prior research suggests that these sharp  
53 transitions (termed *event boundaries*) during an experience help to discretize our experiences into  
54 *events* (Radvansky and Zacks, 2017; Brunec et al., 2018; Heusser et al., 2018a; Clewett and Davachi,  
55 2017; Ezzyat and Davachi, 2011; DuBrow and Davachi, 2013). The interplay between the stable  
56 (within event) and transient (across event) temporal dynamics of an experience also provides a  
57 potential framework for transforming experiences into memories that distill those experiences  
58 down to their essence— i.e., their gists. For example, prior work has shown that event boundaries  
59 can influence how we learn sequences of items (Heusser et al., 2018a; DuBrow and Davachi, 2013),  
60 navigate (Brunec et al., 2018), and remember and understand narratives (Zwaan and Radvansky,  
61 1998; Ezzyat and Davachi, 2011).

62 Here we sought to examine how the temporal dynamics of a “naturalistic” experience were  
63 reflected in participants’ later memories of that experience. We analyzed an open dataset that  
64 comprised behavioral and functional Magnetic Resonance Imaging (fMRI) data collected as par-  
65 ticipants viewed and then verbally recalled an episode of the BBC television series *Sherlock* (Chen  
66 et al., 2017). We developed a computational framework for characterizing the temporal dynamics  
67 of the moment-by-moment content of the episode and of participants’ verbal recalls. Specifically,  
68 we use topic modeling (Blei et al., 2003) to characterize the thematic conceptual (semantic) content  
69 present in each moment of the episode and recalls, and we use Hidden Markov Models (Rabiner,  
70 1989; Baldassano et al., 2017) to discretize the evolving semantic content into events. In this way, we  
71 cast naturalistic experiences (and recalls of those experiences) as *topic trajectories* that describe how  
72 the experiences evolve over time. In other words, the episode’s topic trajectory is a formalization  
73 of its gist. Under this framework, successful remembering entails verbally “traversing” the topic  
74 trajectory of the original episode, thereby reproducing the original episode’s gist. In addition,

75 comparing the shapes of the topic trajectories of the original episode and of participants' retellings  
76 of the episode reveals which aspects of the episode were preserved (or lost) in the translation  
77 into memory. We also identified a network of brain structures whose responses (as participants  
78 watched the episode) reflected the gist of the episode, and a second network whose responses  
79 reflected how participants would later recount the episode.

80 **Results**

81 To characterize the gists of the *Sherlock* episode participants watched and their subsequent recounts  
82 of the episode, we used a topic model (Blei et al., 2003) to discover the latent thematic content  
83 in the video. Topic models take as inputs a vocabulary of words to consider and a collection of text  
84 documents; they return as output two matrices. The first output is a *topics matrix* whose rows are  
85 topics (latent themes) and whose columns correspond to words in the vocabulary. The entries of  
86 the topics matrix define how each word in the vocabulary is weighted by each discovered topic.  
87 For example, a detective-themed topic might weight heavily on words like "crime," and "search."  
88 The second output is a *topic proportions matrix*, with one row per document and one column per  
89 topic. The topic proportions matrix describes which mix topics is reflected in each document.

90 Chen et al. (2017) collected hand-annotated information about each of 1000 (manually identified)  
91 scenes spanning the roughly 45 minute video used in their experiment. This information included:  
92 a brief narrative description of what was happening; whether the scene took place indoors vs.  
93 outdoors; names of any characters on the screen; names of any characters who were in focus in  
94 the camera shot; names of characters who were speaking; the location where the scene took place;  
95 the camera angle (close up, medium, long, etc.); whether or not background music was present;  
96 and other similar details (for a full list of annotated features see *Methods*). We took from these  
97 annotations the union of all unique words (excluding stop words, such as "and," "or," "but," etc.)  
98 across all features and scenes as the "vocabulary" for the topic model. We then concatenated the  
99 sets of words across all features contained in overlapping 50-scene sliding windows, and treated  
100 each 50-scene sequence as a single "document" for the purposes of fitting the topic model. Next,

101 we fit a topic model with (up to)  $K = 100$  topics to this collection of documents. We found that 27  
102 unique topics (with non-zero weights) were sufficient to describe the time-varying content of the  
103 video (see *Methods*; Figs. 1, S2). Note that our approach is similar in some respects to Dynamic Topic  
104 Models (Blei and Lafferty, 2006), in that we sought to characterize how the thematic content of the  
105 episode evolved over time. However, whereas Dynamic Topic Models are designed to characterize  
106 how the properties of *collections* of documents change over time, our sliding window approach  
107 allows us to examine the topic dynamics within a single document (or video). Specifically, our  
108 approach yielded (via the topic proportions matrix) a single *topic vector* for each timepoint of the  
109 episode (we set timepoints to match the acquisition times of the 1976 fMRI volumes collected as  
110 participants viewed the episode).

111 The topics we found were heavily character-focused (e.g., the top-weighted word in each topic  
112 was nearly always a character) and could be roughly divided into themes that were primarily  
113 Sherlock Holmes-focused (Sherlock is the titular character); primarily John Watson-focused (John  
114 is Sherlock's close confidant and assistant); or that involved Sherlock and John interacting (Fig. S2).  
115 Several of the topics were highly similar, which we hypothesized might allow us to distinguish  
116 between subtle narrative differences (if the distinctions between those overlapping topics were  
117 meaningful; also see Fig. S3). The topic vectors for each timepoint were *sparse*, in that only a small  
118 number (usually one or two) of topics tended to be "active" in any given timepoint (Fig. 2A).  
119 Further, the dynamics of the topic activations appeared to exhibit *persistency* (i.e., given that a  
120 topic was active in one timepoint, it was likely to be active in the following timepoint) along with  
121 *occasional rapid changes* (i.e., occasionally topics would appear to spring into or out of existence).  
122 These two properties of the topic dynamics may be seen in the block diagonal structure of the  
123 timepoint-by-timepoint correlation matrix (Fig. 2B). Following Baldassano et al. (2017), we used a  
124 Hidden Markov Model (HMM) to identify the *event boundaries* where the topic activations changed  
125 rapidly (i.e., at the boundaries of the blocks in the correlation matrix; event boundaries identified  
126 by the HMM are outlined in yellow). Part of our model fitting procedure required selecting an  
127 appropriate number of "events" to segment the timeseries into. We used an optimization procedure  
128 to identify the number of events that maximized within-event stability while also minimizing



**Figure 1: Methods overview.** We used hand-annotated descriptions of each moment of video to fit a topic model. Three example video frames and their associated descriptions are displayed (top two rows). Participants later recalled the video (in the third row, we show example recalls of the same three scenes from participant 13). We used the topic model (fit to the annotations) to estimate topic vectors for each moment of video and each sentence the participants recalled. Example topic vectors are displayed in the bottom row (blue: video annotations; green: example participant’s recalls). Three topic dimensions are shown (the highest-weighted topics for each of the three example scenes, respectively). We also show the ten highest-weighted words for each topic. Figure S2 provides a full list of the top 10 words from each of the discovered topics.

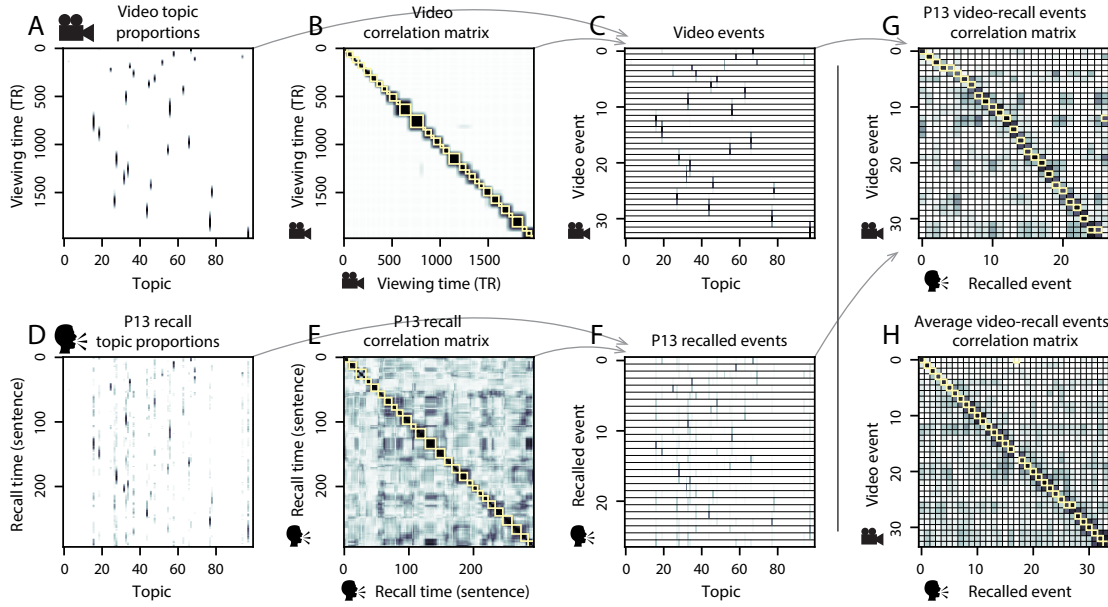


**Figure 2: Modelling naturalistic stimuli and recalls.** All panels: darker colors indicate greater values; range: [0, 1]. **A.** Topic vectors ( $K = 100$ ) for each of the 1976 video timepoints. **B.** Timepoint-by-timepoint correlation matrix of the topic vectors displayed in Panel A. Event boundaries detected by the HMM are denoted in yellow (34 events detected). **C.** Average topic vectors for each of the 34 video events. **D.** Topic vectors for each of 294 sentences spoken by an example participant while recalling the video. **E.** Timepoint-by-timepoint correlation matrix of the topic vectors displayed in Panel D. Event boundaries detected by the HMM are denoted in yellow (27 events detected). **F.** Average topic vectors for each of the 27 recalled events from the example participant. **G.** Correlations between the topic vectors for every pair of video events (Panel C) and recalled events (from the example participant; Panel F). For similar plots for all participants see Figure S6. **H.** Average correlations between each pair of video events and recalled events (across all 17 participants). To create the figure, each recalled event was assigned to the video event with the most correlated topic vector (yellow boxes in panels G and H). The heat maps in each panel were created using Seaborn (Waskom et al., 2016).

129 across-event correlations (see *Methods* for additional details). To create a stable “summary” of the  
 130 video, we computed the average topic vector within each event (Fig. 2C).

131 Given that the time-varying content of the video could be segmented cleanly into discrete  
 132 events, we wondered whether participants’ recalls of the video also displayed a similar structure.  
 133 We applied the same topic model (already trained on the video annotations) to each participant’s  
 134 recalls. Analogous to how we analyzed the time-varying content of the video, to obtain similar  
 135 estimates for participants’ recalls, we treated each (overlapping) 10 sentence “window” of their

transcript as a “document” and then computed the most probable mix of topics reflected in each timepoint’s sentences. This yielded, for each participant, a number-of-sentences by number-of-topics topic proportions matrix that characterized how the topics identified in the original video were reflected in the participant’s recalls. Note that an important feature of our approach is that it allows us to compare participant’s recalls to events from the original video, despite that different participants may have used different language to describe the same event, and that those descriptions may not match the original annotations. This is a huge benefit of projecting the video and recalls into a shared “topic” space. An example topic proportions matrix from one participant’s recalls is shown in Figure 2D.

Although the example participant’s recall topic proportions matrix has some visual similarity to the video topic proportions matrix, the time-varying topic proportions for the example participant’s recalls are not as sparse as for the video (e.g., compare Figs. 2A and D). Similarly, although there do appear to be periods of stability in the recall topic dynamics (e.g., most topics are active or inactive over contiguous blocks of time), the overall timecourses are not as cleanly delineated as the video topics are. To examine these patterns in detail, we computed the timepoint-by-timepoint correlation matrix for the example participant’s recall topic proportions (Fig. 2E). As in the video correlation matrix (Fig. 2B), the example participant’s recall correlation matrix has a strong block diagonal structure, indicating that their recalls are discretized into separated events. As for the video correlation matrix, we can use an HMM, along with the aforementioned number-of-events optimization procedure (also see *Methods*) to determine how many events are reflected in the participant’s recalls and where specifically the event boundaries fall (outlined in yellow). We carried out a similar analysis on all 17 participants’ recall topic proportions matrices (Fig. S5).

Two clear patterns emerged from this set of analyses. First, although every individual participant’s recalls could be segmented into discrete events (i.e., every individual participant’s recall correlation matrix exhibited clear block diagonal structure; Fig. S5), each participant appeared to have a unique *recall resolution*, reflected in the sizes of those blocks. For example, some participants’ recall topic proportions segmented into just a few events (e.g., Participants P1, P4, and P15), while others’ recalls segmented into many shorter duration events (e.g., Participants P12, P13, and P17).

164 This suggests that different participants may be recalling the video with different levels of detail–  
165 e.g., some might touch on just the major plot points, whereas others might attempt to recall every  
166 minor scene. The second clear pattern present in every individual participant’s recall correlation  
167 matrix is that, unlike in the video correlation matrix, there are substantial off-diagonal correlations  
168 in participant’s recalls. Whereas each event in the original video (was largely) separable from the  
169 others (Fig. 2B), in transforming those separable events into memory participants appear to be  
170 integrating *across* different events, blending elements of previously recalled and not-yet-recalled  
171 events into each newly recalled event (Figs. 2D, S5; also see Manning et al., 2011; Howard et al.,  
172 2012).

173 The above results indicate that both the structure of the original video and participants’ recalls  
174 of the video exhibit event boundaries that can be identified automatically by characterizing the  
175 dynamic content using a shared topic model and segmenting the content into events using HMMs.  
176 Next we asked whether some correspondence might be made between the specific content of  
177 the events the participants experienced in the video, and the events they later recalled. One  
178 approach to linking the experienced (video) and recalled events is to label each recalled event as  
179 matching the video event with the most similar (i.e., most highly correlated) topic vector (Figs. 2G,  
180 S6). This yields a sequence of “presented” events from the original video, and a sequence of  
181 (potentially differently ordered) “recalled” events for each participant. Analogous to classic list-  
182 learning studies, we can then examine participants’ recall sequences by asking which events  
183 they tended to recall first (probability of first recall; Fig. S4A; Welch and Burnett, 1924; Postman  
184 and Phillips, 1965; Atkinson and Shiffrin, 1968); how participants most often transition between  
185 recalls of the events as a function of the temporal distance between them (lag-conditional response  
186 probability; Fig. S4B; Kahana, 1996); and which events they were likely to remember overall (serial  
187 position recall analyses; Fig. S4C; Murdock, 1962). In list-learning studies, this set of three analyses  
188 may be used to gain a nearly complete view into the sequences of recalls participants made (e.g.,  
189 Kahana, 2012). Extending these analyses to apply to naturalistic stimuli and recall (Heusser et al.,  
190 2017) highlights that, in naturalistic recall, these analyses provide a wholly incomplete picture: they  
191 leave out any attempt to quantify participants’ abilities to capture the *content* of what occurred in

192 the video— their only experimental instruction!

193 The dynamic content of the video and participants' recalls is quantified in the corresponding  
194 topic proportion matrices. However, it is difficult to gain deep insights into that content solely  
195 by examining the topic proportion matrices (e.g., Figs. 2A, D) or the corresponding correlation  
196 matrices (Figs. 2B, E, S5). To visualize the time-varying high-dimensional content in a more  
197 intuitive way (Heusser et al., 2018b) we projected the topic proportions matrices onto a two-  
198 dimensional space using Uniform Manifold Approximation and Projection (UMAP; McInnes and  
199 Healy, 2018). In this lower-dimensional space, each point represents a single video or recall event,  
200 and the distances between the points reflect the distances between the events' associated topic  
201 vectors (Fig. 3).

202 Visual inspection of the video and recall topic trajectories reveals a striking pattern. First,  
203 the topic trajectory of the video (which reflects its dynamic content; Fig. 3A) is captured nearly  
204 perfectly by the averaged topic trajectories of participants' recalls (Fig. 3B). To assess the consistency  
205 of these recall trajectories across participants, we asked: given that a participant's recall trajectory  
206 had entered a particular location in topic space, could the position of their *next* recalled event  
207 be predicted reliably? For each location in topic space, we computed the set of line segments  
208 connecting successively recalled events (across all participants) that intersected that location (see  
209 *Methods* for additional details). We then computed (for each location) the distribution of angles  
210 formed by the lines defined by those line segments and a fixed reference line (the *x*-axis). Rayleigh  
211 tests revealed the set of locations in topic space at which these across-participant distributions  
212 exhibited reliable peaks (blue arrows in Fig. 3B reflect significant peaks at  $p < 0.05$ , corrected). We  
213 observed that the locations traversed by nearly the entire video trajectory exhibited such peaks.  
214 In other words, participants exhibited similar trajectories that also matched the trajectory of the  
215 original video (Fig. 3C). This is especially notable when considering the fact that the number of  
216 events participants recalled (dots in Fig. 3C) varied considerably across people, and that every  
217 participant used different words to describe what they had remembered happening in the video.  
218 Differences in the numbers of remembered events appear in participants' trajectories as differences  
219 in the sampling resolution along the trajectory. We note that this framework also provides a

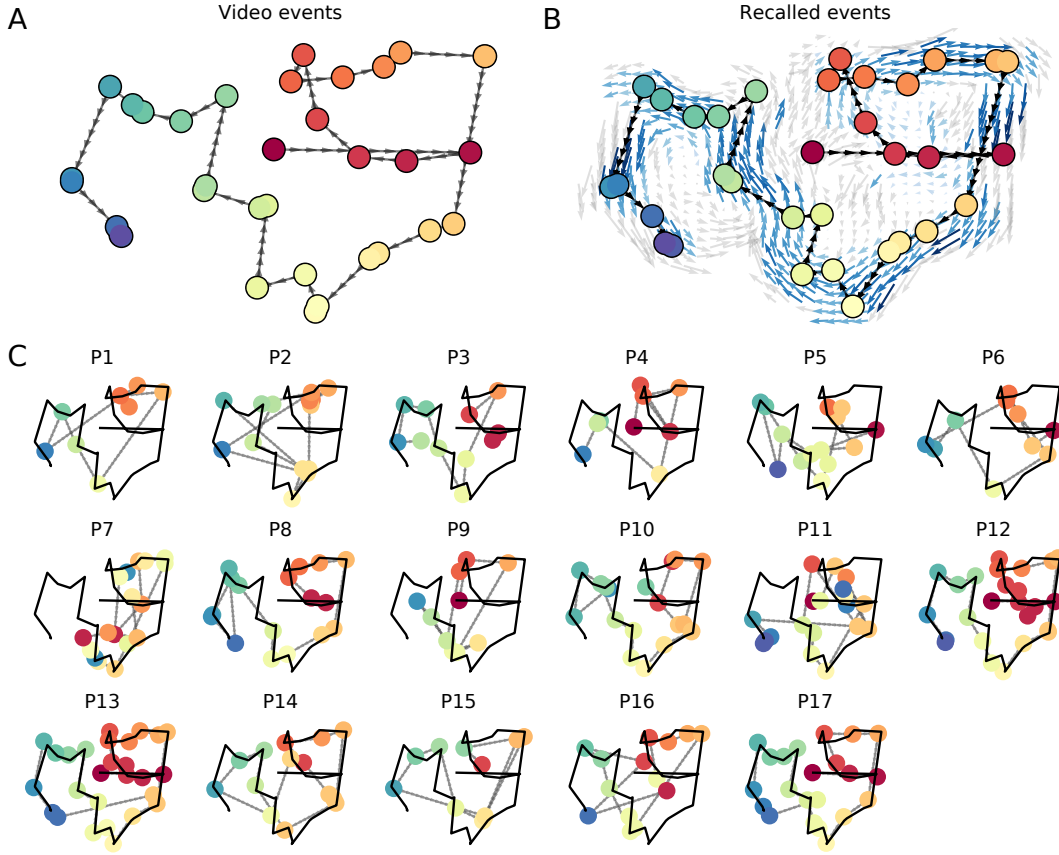


**Figure 3: Trajectories through topic space capture the dynamic content of the video and recalls.** All panels: the topic proportion matrices have been projected onto a shared two-dimensional space using UMAP. **A.** The two-dimensional topic trajectory taken by the episode of *Sherlock*. Each dot indicates an event identified using the HMM (see *Methods*); the dot colors denote the order of the events (early events are in red; later events are in blue), and the connecting lines indicate the transitions between successive events. **B.** The average two-dimensional trajectory captured by participants' recall sequences, with the same format and coloring as the trajectory in Panel A. To compute the event positions, we matched each recalled event with an event from the original video (see *Results*), and then we averaged the positions of all events with the same label. The arrows reflect the average transition direction through topic space taken by any participants whose trajectories crossed that part of topic space; blue denotes reliable agreement across participants via a Rayleigh test ( $p < 0.05$ , corrected). **C.** The recall topic trajectories (gray) taken by each individual participant (P1–P17). The video's trajectory is shown in black for reference. (Same format and coloring as Panel A.)

means of detangling classic “proportion recalled” measures (i.e., the proportion of video events referenced in participants’ recalls) from participants’ abilities to recapitulate the full gist of the original video (i.e., the similarity in the shape of the original video trajectory and that defined by each participant’s recounting of the video).

Because our analysis framework projects the dynamic video content and participants’ recalls onto a shared topic space, and because the dimensions of that space are known (i.e., each topic dimension is a set of weights over words in the vocabulary; Fig. S2), we can examine the topic trajectories to understand which specific content was remembered well (or poorly). For each video event, we can ask: what was the average correlation (across participants) between the video event’s topic vector and the closest matching recall event topic vectors from each participant? This yields a single correlation coefficient for each video event, describing how closely participants’ recalls of the event tended to reliably capture its content (Fig. 4A). (We also examined how different comparisons between each video event’s topic vector and the corresponding recall event topic vectors related to hand-annotated characterizations of memory performance; see *Supporting Information*). Given this summary of which events were recalled reliably (or not), we next asked whether the better-remembered or worse-remembered events tended to reflect particular topics. We computed a weighted average of the topic vectors for each video event, where the weights reflected how reliably each event was recalled. To visualize the result, we created a “wordle” image (Mueller et al., 2018) where words weighted more heavily by better-remembered topics appear in a larger font (Fig. 4B, green box). Events that reflected topics weighting heavily on characters like “Sherlock” and “John” (i.e., the main characters) and locations like “221b Baker Street” (i.e., a major recurring location and the address of the flat that Sherlock and John share) were best remembered. An analogous analysis revealed which themes were poorly remembered. Here in computing the weighted average over events’ topic vectors we weighted each event in *inverse* proportion to how well it was remembered (Fig. 4B, red box). This revealed that events with relatively minor characters such as “Mike,” “Jeffrey,” and “Molly,” as well as less-integral plot locations (e.g., “hospital” and “office”) were least well-remembered. This suggests that what is retained in memory are the major plot elements (i.e., the overall “gist” of what happened), whereas the more minor details are prone to pruning.

248 In addition to constructing overall summaries, assessing the video and recall topic vectors from  
249 individual recalls can provide further insights. Specifically, for any given event we can construct  
250 two wordles: one from the original video event's topic vector, and a second from the average topic  
251 vectors produced by all participants' recalls of that event. We can then examine those wordles  
252 visually to gain an intuition for which aspects of the video event were recapitulated in participants'  
253 recalls of that event. Several example wordles are displayed in Figure 4C (wordles from the three  
254 best-remembered events are circled in green; wordles from the three worst-remembered events  
255 are circled in red). Using wordles to visually compare the topical content of each video event and  
256 the (average) corresponding recall event reveals the specific content from the specific events that  
257 is reliably retained in the transformation into memory (green events) or not (red events).

258 The results thus far inform us about which aspects of the dynamic content in the episode  
259 participants watched were preserved or altered in participants' memories of the episode. We next  
260 carried out a series of analyses aimed at understanding which brain structures might implement  
261 these processes. In one analysis we sought to identify which brain structures were sensitive  
262 to the video's dynamic content, as characterized by its topic trajectory. Specifically, we used a  
263 searchlight procedure to identify the extent to which each cluster of voxels exhibited a timecourse  
264 (as the participants watched the video) whose temporal correlation matrix matched the temporal  
265 correlation matrix of the original video's topic proportion matrix (Fig. 2B). As shown in Figure 5A,  
266 the analysis revealed a network of regions including bilateral frontal cortex and cingulate cortex,  
267 suggesting that these regions may play a role in maintaining information relevant to the narrative  
268 structure of the video. In a second analysis, we sought to identify which brain structures' responses  
269 (while viewing the video) reflected how each participant would later *recall* the video. We used an  
270 analogous searchlight procedure to identify clusters of voxels whose temporal correlation matrices  
271 reflected the temporal correlation matrix of the topic proportions for each individual's recalls  
272 (Figs. 2D, S5). As shown in Figure 5B, the analysis revealed a network of regions including the  
273 ventromedial prefrontal cortex (vmPFC), anterior cingulate cortex, and right medial temporal  
274 lobe (rMTL), suggesting that these regions may play a role in transforming each individual's  
275 experience into memory. In identifying regions whose responses to ongoing experiences reflect

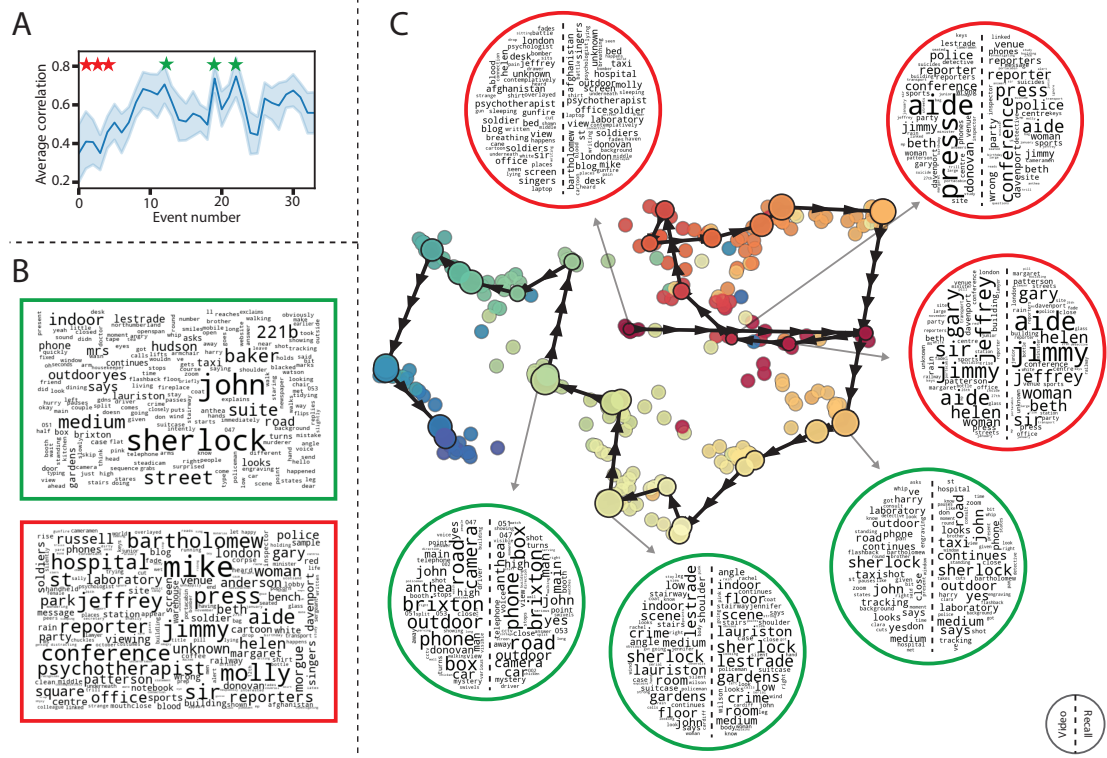


**Figure 4: Transforming experience into memory.** **A.** Average correlations (across participants) between the topic vectors from each video event and the closest-matching recall events. Error bars denote bootstrap-derived across-participant 95% confidence intervals. The stars denote the three best-remembered events (green) and worst-remembered events (red). **B.** Wordles comprising the top 200 highest-weighted words reflected in the weighted-average topic vector across video events. Green: video events were weighted by how well the topic vectors derived from recalls of those events matched the video events' topic vectors (Panel A). Red: video events were weighted by the inverse of how well their topic vectors matched the recalled topic vectors. **C.** The set of all video and recall events is projected onto the two-dimensional space derived in Figure 3. The dots outlined in black denote video events (dot size reflects the average correlation between the video event's topic vector and the topic vectors from the closest matching recalled events from each participant; bigger dots denote stronger correlations). The dots without black outlines denote recalled events. All dots are colored using the same scheme as Figure 3A. Wordles for several example events are displayed (green: three best-remembered events; red: three worst-remembered events). Within each circular wordle, the left side displays words associated with the topic vector for the video event, and the right side displays words associated with the (average) recall event topic vector, across all recall events matched to the given video event.

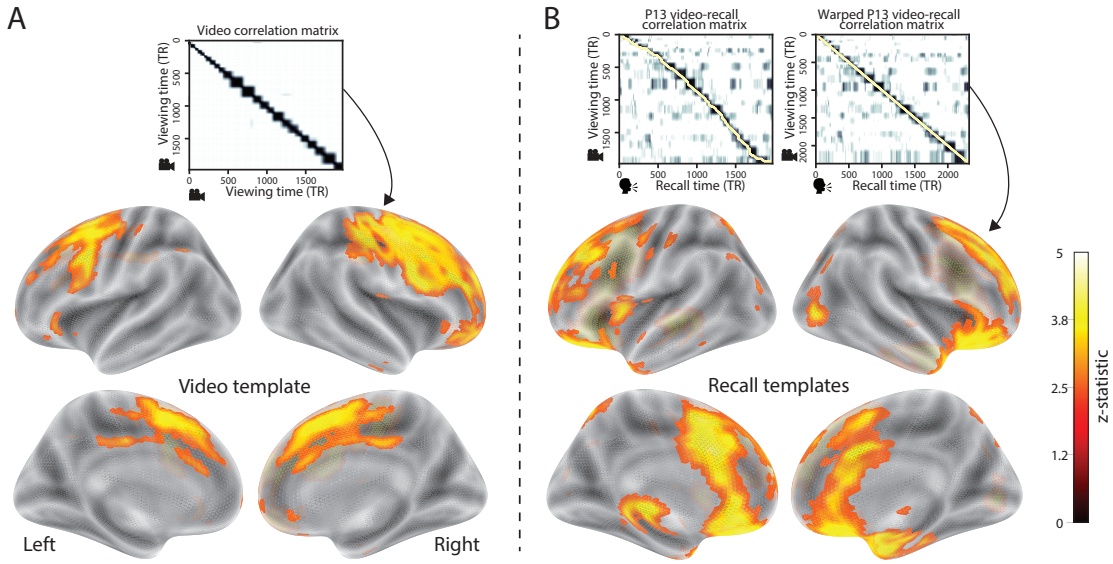


**Figure 5: Brain structures that underlie the transformation of experience into memory.** **A.** We searched for regions whose responses (as participants watched the video) matched the temporal correlation matrix of the video topic proportions. These regions are sensitive to the narrative structure of the video. **B.** We searched for regions whose responses (as participants watched the video) matched the temporal correlation matrix of the topic proportions derived from each individual's later recall of video. These regions are sensitive to how the narrative structure of the video is transformed into a memory of the video. Both panels: the maps are thresholded at  $p < 0.05$ , corrected.

276 how those experiences will be remembered later, this latter analysis extends classic *subsequent*  
 277 *memory analyses* (e.g., Paller and Wagner, 2002) to domain of naturalistic stimuli.

## 278 Discussion

279 Our work casts remembering as reproducing (behaviorally and neurally) the topic trajectory, or  
 280 “gist,” of the original experience. This view draws inspiration from prior work aimed at elucidating  
 281 the neural and behavioral underpinnings of how we process dynamic naturalistic experiences  
 282 and remember them later. One approach to identifying neural responses to naturalistic stimuli  
 283 (including experiences) entails building a model of the stimulus and searching for brain regions  
 284 whose responses are consistent with the model. In prior work, a series of studies from Uri  
 285 Hasson’s group (Lerner et al., 2011; Simony et al., 2016; Chen et al., 2017; Baldassano et al., 2017;

Zadbood et al., 2017) have extended this approach with a clever twist. Rather than building an explicit stimulus model, these studies instead search for brain responses (while experiencing the stimulus) that are reliably similar across individuals. So called *inter-subject correlation* (ISC) and *inter-subject functional connectivity* (ISFC) analyses effectively treat other people's brain responses to the stimulus as a "model" of how its features change over time. By contrast, in our present work we used topic models and HMMs to construct an explicit stimulus model (i.e., the topic trajectory of the video). When we searched for brain structures whose responses are consistent with the video's topic trajectory, we identified a network of structures that overlapped strongly with the "long temporal receptive window" network reported by the Hasson group (e.g., compare our Fig. 5A with the map of long temporal receptive window voxels in Lerner et al., 2011). This provides support for the notion that part of the long temporal receptive window network may be maintaining an explicit model of the stimulus dynamics. When we performed a similar analysis after swapping out the video's topic trajectory with the recall topic trajectories of each individual participant, this allowed us to identify brain regions whose responses (as the participants viewed the video) reflected how the video trajectory would be transformed in memory (as reflected by the recall topic trajectories). The analysis revealed that the rMTL and vmPFC may play a role in this person-specific transformation from experience into memory. The role of the MTL in episodic memory encoding has been well-reported (e.g., Paller and Wagner, 2002; Davachi et al., 2003; Ranganath et al., 2004; Davachi, 2006). Prior work has also implicated the medial prefrontal cortex in representing "schema" knowledge (i.e., general knowledge about the format of an ongoing experience given prior similar experiences; van Kesteren et al., 2012; Schlichting and Preston, 2015; Gilboa and Marlatte, 2017; Spalding et al., 2018). Integrating across our study and this prior work, one interpretation is that the person-specific transformations mediated (or represented) by the rMTL and vmPFC may reflect schema knowledge being leveraged, formed, or updated, incorporating ongoing experience into previously acquired knowledge.

Our work has broad implications for how we characterize and assess memory in real-world settings such as the classroom or physician's office. For example, the most commonly used classroom evaluation tools involve computing the proportion of correctly answered exam questions. Our

314 work indicates that this approach is only loosely related to what educators might really want to  
315 measure: how well did the students understand the key ideas presented in the course? One could  
316 apply the computational framework we developed to construct topic trajectories for the video and  
317 participants' recalls to build explicit content models of the course material and exam questions.  
318 This approach would provide a more nuanced and specific view into which aspects of the material  
319 students had learned well (or poorly). In clinical settings, memory measures that incorporate such  
320 explicit content models might also provide more direct evaluations of patients' memories.

## 321 **Methods**

### 322 **Experimental design and data collection**

323 Data were collected by Chen et al. (2017). In brief, participants ( $n = 17$ ) viewed the first 48 minutes  
324 of "A Study in Pink", the first episode of the BBC television series *Sherlock*, while fMRI volumes  
325 were collected (TR = 1500 ms). The stimulus was divided into a 23 min (946 TR) and a 25 min  
326 (1030 TR) segment to mitigate technical issues related to the scanner. After finishing the clip,  
327 participants were instructed to (quoting from Chen et al., 2017) "describe what they recalled of  
328 the [episode] in as much detail as they could, to try to recount events in the original order they  
329 were viewed in, and to speak for at least 10 minutes if possible but that longer was better. They  
330 were told that completeness and detail were more important than temporal order, and that if at  
331 any point they realized they had missed something, to return to it. Participants were then allowed  
332 to speak for as long as they wished, and verbally indicated when they were finished (e.g., 'I'm  
333 done')." For additional details about the experimental procedure and scanning parameters see  
334 Chen et al. (2017).

335 After preprocessing the fMRI data and warping the images into a standard (3 mm<sup>3</sup> MNI) space,  
336 the voxel activations were z-scored (within voxel) and spatially smoothed using a 6 mm (full width  
337 at half maximum) Gaussian kernel. The fMRI data were also cropped so that all video-viewing  
338 data were aligned across participants. This included a constant 3 TR (4.5 s) shift to account for the

339 lag in the hemodynamic response. (All of these preprocessing steps followed Chen et al., 2017,  
340 where additional details may be found.)

341 **Data availability**

342 The behavioral and fMRI data we analyzed are available online [here](#).

343 **Statistics**

344 All statistical tests we performed were two-sided.

345 **Modeling the dynamic content of the video and recall transcripts**

346 **Topic modeling**

347 The input to the topic model we trained to characterize the dynamic content of the video comprised  
348 hand-generated annotations of each of 1000 scenes spanning the video clip (generated by Chen  
349 et al., 2017). The features included: narrative details (a sentence or two describing what happened  
350 in that scene); whether the scene took place indoors or outdoors; names of any characters that  
351 appeared in the scene; name(s) of characters in camera focus; name(s) of characters who were  
352 speaking in the scene; the location (in the story) that the scene took place; camera angle (close  
353 up, medium, long, top, tracking, over the shoulder, etc.); whether music was playing in the  
354 scene or not; and a transcription of any on-screen text. We concatenated the text for all of these  
355 features within each segment, creating a “bag of words” describing each scene. We then re-  
356 organized the text descriptions into overlapping sliding windows spanning 50 scenes each. In  
357 other words, the first text sample comprised the combined text from the first 50 scenes (i.e., 1–50),  
358 the second comprised the text from scenes 2–51, and so on. We trained our model using these  
359 overlapping text samples with `scikit-learn` (version 0.19.1; Pedregosa et al., 2011), called from  
360 our high-dimensional visualization and text analysis software, `HyperTools` (Heusser et al., 2018b).  
361 Specifically, we use the `CountVectorizer` class to transform the text from each scene into a vector of  
362 word counts (using the union of all words across all scenes as the “vocabulary,” excluding English

363 stop words); this yields a number-of-scenes by number-of-words *word count* matrix. We then  
364 use the `LatentDirichletAllocation` class (`topics=100, method='batch'`) to fit a topic model (Blei  
365 et al., 2003) to the word count matrix, yielding a number-of-scenes (1000) by number-of-topics  
366 (100) *topic proportions* matrix. The topic proportions matrix describes which mix of topics (latent  
367 themes) is present in each scene. Next, we transformed the topic proportions matrix to match the  
368 1976 fMRI volume acquisition times. For each fMRI volume, we took the topic proportions from  
369 whatever scene was displayed for most of that volume's 1500 ms acquisition time. This yielded a  
370 new number-of-TRs (1976) by number-of-topics (100) topic proportions matrix.

371 We created similar topic proportions matrices using hand-annotated transcripts of each partici-  
372 pant's recall of the video (annotated by Chen et al., 2017). We tokenized the transcript into a list of  
373 sentences, and then re-organized the list into overlapping sliding windows spanning 10 sentences  
374 each; in turn we transformed each window's sentences into a word count vector (using the same  
375 vocabulary as for the video model). We then used the topic model already trained on the video  
376 scenes to compute the most probable topic proportions for each sliding window. This yielded a  
377 number-of-sentences (range: 68–294) by number-of-topics (100) topic proportions matrix, for each  
378 participant. These reflected the dynamic content of each participant's recalls. Note: for details  
379 on how we selected the video and recall window lengths and number of topics, see *Supporting*  
380 *Information* and Figure S1.

### 381 **Parsing topic trajectories into events using Hidden Markov Models**

382 We parsed the topic trajectories of the video and participants' recalls into events using Hidden  
383 Markov Models (Rabiner, 1989). Given the topic proportions matrix (describing the mix of topics  
384 at each timepoint) and a number of states,  $K$ , an HMM recovers the set of state transitions that  
385 segments the timeseries into  $K$  discrete states. Following Baldassano et al. (2017), we imposed an  
386 additional set of constraints on the discovered state transitions that ensured that each state was  
387 encountered exactly once (i.e., never repeated). We used the BrainIAK toolbox (Capota et al., 2017)  
388 to implement this segmentation.

389 We used an optimization procedure to select the appropriate  $K$  for each topic proportions

390 matrix. Specifically, we computed (for each matrix)

$$\operatorname{argmax}_K \left[ \frac{a}{b} - \frac{K}{\alpha} \right],$$

391 where  $a$  was the average correlation between the topic vectors of timepoints within the same state;  
392  $b$  was the average correlation between the topic vectors of timepoints within *different* states; and  
393  $\alpha$  was a regularization parameter that we set to 5 times the window length (i.e., 250 scenes for  
394 the video topic trajectory and 50 sentences for the recall topic trajectories). Figure 2B displays the  
395 event boundaries returned for the video, and Figure S5 displays the event boundaries returned  
396 for each participant's recalls. After obtaining these event boundaries, we created stable estimates  
397 of each topic proportions matrix by averaging the topic vectors within each event. This yielded a  
398 number-of-events by number-of-topics matrix for the video and recalls from each participant.

### 399 **Visualizing the video and recall topic trajectories**

400 We used the UMAP algorithm (McInnes and Healy, 2018) to project the 100-dimensional topic space  
401 onto a two-dimensional space for visualization (Figs. 3, 4). To ensure that all of the trajectories were  
402 projected onto the *same* lower dimensional space, we computed the low-dimensional embedding  
403 on a "stacked" matrix created by vertically concatenating the events-by-topics topic proportions  
404 matrices for the video and all 17 participants' recalls. We then divided the rows of the result (a  
405 total-number-of-events by two matrix) back into separate matrices for the video topic trajectory  
406 and the trajectories for each participant's recalls (Fig. 3). This general approach for discovering  
407 a shared low-dimensional embedding for a collections of high-dimensional observations follows  
408 Heusser et al. (2018b).

### 409 **Estimating the consistency of flow through topic space across participants**

410 In Figure 3B, we present an analysis aimed at characterizing locations in topic space that dif-  
411 ferent participants move through in a consistent way (via their recall topic trajectories). The  
412 two-dimensional topic space used in our visualizations (Fig. 3) ranged from -5 to 5 (arbitrary) units

413 in the  $x$  dimension and from -6.5 to 2 units in the  $y$  dimension. We divided this space into a grid  
414 of vertices spaced 0.25 units apart. For each vertex, we examined the set of line segments formed  
415 by connecting each pair successively recalled events, across all participants, that passed within 0.5  
416 units. We computed the distribution of angles formed by those segments and the  $x$ -axis, and used a  
417 Rayleigh test to determine whether the distribution of angles was reliably “peaked” (i.e., consistent  
418 across all transitions that passed through that local portion of topic space). To create Figure 3B we  
419 drew an arrow originating from each grid vertex, pointing in the direction of the average angle  
420 formed by line segments that passed within 0.5 units. We set the arrow lengths to be inversely  
421 proportional to the  $p$ -values of the Rayleigh tests at each vertex. Specifically, for each vertex we  
422 converted all of the angles of segments that passed within 0.5 units to unit vectors, and we set  
423 the arrow lengths at each vertex proportional to the length of the (circular) mean vector. We also  
424 indicated any significant results ( $p < 0.05$ , corrected using the Benjamani-Hochberg procedure) by  
425 coloring the arrows in blue (darker blue denotes a lower  $p$ -value, i.e., a longer mean vector); all  
426 tests with  $p \geq 0.05$  are displayed in gray and given a lower opacity value.

## 427 Searchlight fMRI analyses

428 In Figure 5, we present two analyses aimed at identifying brain structures whose responses (as  
429 participants viewed the video) exhibited particular temporal correlations. We developed a search-  
430 light analysis whereby we constructed a cube centered on each voxel (radius: 5 voxels). For each  
431 of these cubes, we computed the temporal correlation matrix of the voxel responses during video  
432 viewing. Specifically, for each of the 1976 volumes collected during video viewing, we correlated  
433 the activity patterns in the given cube with the activity patterns (in the same cube) collected during  
434 every other timepoint. This yielded a 1976 by 1976 correlation matrix for each cube.

435 Next, we constructed two sets of “template” matrices: one reflected the video’s topic trajectory  
436 and the other reflected each participant’s recall topic trajectory. To construct the video template, we  
437 computed the correlations between the topic proportions estimated for every pair of TRs (prior to  
438 segmenting the trajectory into discrete events; i.e., the correlation matrix shown in Figs. 2B and 5A).  
439 We constructed similar temporal correlation matrices for each participant’s recall topic trajectory

440 (Figs. 2D, S5). However, to correct for length differences and potential non-linear transformations  
441 between viewing time and recall time, we first used dynamic time warping (Berndt and Clifford,  
442 1994) to temporally align participants' recall topic trajectories with the video topic trajectory (an  
443 example correlation matrix before and after warping is shown in Fig. 5B). This yielded a 1976 by  
444 1976 correlation matrix for the video template and for each participant's recall template.

445 To determine which (cubes of) voxel responses reliably matched the video template, we cor-  
446 related the upper triangle of the voxel correlation matrix for each cube with the upper triangle  
447 of the video template matrix (Kriegeskorte et al., 2008). This yielded, for each participant, a  
448 single correlation value. We computed the average (Fisher  $z$ -transformed) correlation coefficient  
449 across participants. We used a permutation-based procedure to assess significance, whereby we  
450 re-computed the average correlations for each of 100 "null" video templates (constructed by circu-  
451 larly shifting the template by a random number of timepoints). (For each permutation, the same  
452 shift was used for all participants.) We then estimated a  $p$ -value by computing the proportion of  
453 shifted correlations that were larger than the observed (unshifted) correlation. To create the map  
454 in Figure 5A we thresholded out any voxels whose correlation values fell below the 95<sup>th</sup> percentile  
455 of the permutation-derived null distribution.

456 We used a similar procedure to identify which voxels' responses reflected the recall templates.  
457 For each participant, we correlated the upper triangle of the correlation matrix for each cube of  
458 voxels with their (time warped) recall correlation matrix. As in the video template analysis this  
459 yielded a single correlation coefficient for each participant. However, whereas the video analysis  
460 compared every participant's responses to the same template, here the recall templates were  
461 unique for each participant. We computed the average  $z$ -transformed correlation coefficient across  
462 participants, and used the same permutation procedure we developed for the video responses to  
463 assess significant correlations. To create the map in Figure 5B we thresholded out any voxels whose  
464 correlation values fell below the 95<sup>th</sup> percentile of the permutation-derived null distribution.

465 **References**

- 466 Atkinson, R. C. and Shiffrin, R. M. (1968). Human memory: A proposed system and its control  
467 processes. In Spence, K. W. and Spence, J. T., editors, *The psychology of learning and motivation*,  
468 volume 2, pages 89–105. Academic Press, New York.
- 469 Baldassano, C., Chen, J., Zadbood, A., Pillow, J. W., Hasson, U., and Norman, K. A. (2017).  
470 Discovering event structure in continuous narrative perception and memory. *Neuron*, 95(3):709–  
471 721.
- 472 Berndt, D. J. and Clifford, J. (1994). Using dynamic time warping to find patterns in time series. In  
473 *KDD workshop*, volume 10, pages 359–370.
- 474 Blei, D. M. and Lafferty, J. D. (2006). Dynamic topic models. In *Proceedings of the 23rd International  
475 Conference on Machine Learning*, ICML '06, pages 113–120, New York, NY, US. ACM.
- 476 Blei, D. M., Ng, A. Y., and Jordan, M. I. (2003). Latent dirichlet allocation. *Journal of Machine  
477 Learning Research*, 3:993 – 1022.
- 478 Brunec, I. K., Moscovitch, M. M., and Barense, M. D. (2018). Boundaries shape cognitive represen-  
479 tations of spaces and events. *Trends in Cognitive Sciences*, 22(7):637–650.
- 480 Capota, M., Turek, J., Chen, P.-H., Zhu, X., Manning, J. R., Sundaram, N., Keller, B., Wang, Y., and  
481 Shin, Y. S. (2017). Brain imaging analysis kit.
- 482 Chen, J., Leong, Y. C., Norman, K. A., and Hasson, U. (2017). Shared experience, shared memory: a  
483 common structure for brain activity during naturalistic recall shared experience, shared memory:  
484 a common structure for brain activity during naturalistic recall. *Nature Neuroscience*, 20(1):115–  
485 125.
- 486 Clewett, D. and Davachi, L. (2017). The ebb and flow of experience determines the temporal  
487 structure of memory. *Curr Opin Behav Sci*, 17:186–193.
- 488 Davachi, L. (2006). Item, context and relational episodic encoding in humans. *Current Opinion in  
489 Neurobiology*, 16(6):693—700.

- 490 Davachi, L., Mitchell, J. P., and Wagner, A. D. (2003). Multiple routes to memory: distinct medial  
491 temporal lobe processes build item and source memories. *Proceedings of the National Academy of*  
492 *Sciences, USA*, 100(4):2157 – 2162.
- 493 DuBrow, S. and Davachi, L. (2013). The influence of contextual boundaries on memory for the  
494 sequential order of events. *Journal of Experimental Psychology: General*, 142(4):1277–1286.
- 495 Ezzyat, Y. and Davachi, L. (2011). What constitutes an episode in episodic memory? *Psychological*  
496 *Science*, 22(2):243–252.
- 497 Gilboa, A. and Marlatte, H. (2017). Neurobiology of schemas and schema-mediated memory.  
498 *Trends Cogn Sci*, 21(8):618–631.
- 499 Heusser, A. C., Ezzyat, Y., Shiff, I., and Davachi, L. (2018a). Perceptual boundaries cause mnemonic  
500 trade-offs between local boundary processing and across-trial associative binding. *Journal of*  
501 *Experimental Psychology Learning, Memory, and Cognition*, 44(7):1075–1090.
- 502 Heusser, A. C., Fitzpatrick, P. C., Field, C. E., Ziman, K., and Manning, J. R. (2017). Quail: a  
503 Python toolbox for analyzing and plotting free recall data. *The Journal of Open Source Software*,  
504 10.21105/joss.00424.
- 505 Heusser, A. C., Ziman, K., Owen, L. L. W., and Manning, J. R. (2018b). HyperTools: a Python  
506 toolbox for gaining geometric insights into high-dimensional data. *Journal of Machine Learning*  
507 *Research*, 18(152):1–6.
- 508 Howard, M. W. and Kahana, M. J. (2002). A distributed representation of temporal context. *Journal*  
509 *of Mathematical Psychology*, 46:269–299.
- 510 Howard, M. W., MacDonald, C. J., Tiganj, Z., Shankar, K. H., Du, Q., Hasselmo, M. E., and H., E.  
511 (2014). A unified mathematical framework for coding time, space, and sequences in the medial  
512 temporal lobe. *Journal of Neuroscience*, 34(13):4692–4707.
- 513 Howard, M. W., Viskontas, I. V., Shankar, K. H., and Fried, I. (2012). Ensembles of human MTL  
514 neurons “jump back in time” in response to a repeated stimulus. *Hippocampus*, 22:1833–1847.

- 515 Huk, A., Bonnen, K., and He, B. J. (2018). Beyond trial-based paradigms: continuous behavior, on-  
516 going neural activity, and naturalistic stimuli. *Journal of Neuroscience*, 10.1523/JNEUROSCI.1920-  
517 17.2018.
- 518 Kahana, M. J. (1996). Associative retrieval processes in free recall. *Memory & Cognition*, 24:103–109.
- 519 Kahana, M. J. (2012). *Foundations of Human Memory*. Oxford University Press, New York, NY.
- 520 Koriat, A. and Goldsmith, M. (1994). Memory in naturalistic and laboratory contexts: distin-  
521 guishing accuracy-oriented and quantity-oriented approaches to memory assessment. *Journal of*  
522 *Experimental Psychology: General*, 123(3):297–315.
- 523 Kriegeskorte, N., Mur, M., and Bandettini, P. (2008). Representational similarity analysis – con-  
524 nnecting the branches of systems neuroscience. *Frontiers in Systems Neuroscience*, 2:1 – 28.
- 525 Lerner, Y., Honey, C. J., Silbert, L. J., and Hasson, U. (2011). Topographic mapping of a hierarchy  
526 of temporal receptive windows using a narrated story. *Journal of Neuroscience*, 31(8):2906–2915.
- 527 Manning, J. R., Norman, K. A., and Kahana, M. J. (2015). The role of context in episodic memory.  
528 In Gazzaniga, M., editor, *The Cognitive Neurosciences, Fifth edition*, pages 557–566. MIT Press.
- 529 Manning, J. R., Polyn, S. M., Baltuch, G., Litt, B., and Kahana, M. J. (2011). Oscillatory patterns  
530 in temporal lobe reveal context reinstatement during memory search. *Proceedings of the National*  
531 *Academy of Sciences, USA*, 108(31):12893–12897.
- 532 McInnes, L. and Healy, J. (2018). UMAP: Uniform manifold approximation and projection for  
533 dimension reduction. *arXiv*, 1802(03426).
- 534 Mueller, A., Fillion-Robin, J.-C., Boidol, R., Tian, F., Nechifor, P., yoonsubKim, Peter, Rampin, R.,  
535 Corvellec, M., Medina, J., Dai, Y., Petrushev, B., Langner, K. M., Hong, Alessio, Ozsvald, I.,  
536 vkolmakov, Jones, T., Bailey, E., Rho, V., IgorAPM, Roy, D., May, C., foobuzz, Piyush, Seong,  
537 L. K., Goey, J. V., Smith, J. S., Gus, and Mai, F. (2018). WordCloud 1.5.0: a little word cloud  
538 generator in Python. *Zenodo*, <https://zenodo.org/record/1322068#.W4tPKZNKh24>.

- 539 Murdock, B. B. (1962). The serial position effect of free recall. *Journal of Experimental Psychology*,  
540 64:482–488.
- 541 Paller, K. A. and Wagner, A. D. (2002). Observing the transformation of experience into memory.  
542 *Trends in Cognitive Sciences*, 6(2):93–102.
- 543 Pedregosa, F., Varoquaux, G., Gramfort, A., Michel, V., Thirion, B., Grisel, O., Blondel, M., Pretten-  
544 hofer, P., Weiss, R., Dubourg, V., Vanderplas, J., Passos, A., Cournapeau, D., Brucher, M., Perrot,  
545 M., and Duchesnay, E. (2011). Scikit-learn: Machine learning in Python. *Journal of Machine  
546 Learning Research*, 12:2825–2830.
- 547 Postman, L. and Phillips, L. W. (1965). Short-term temporal changes in free recall. *Quarterly Journal  
548 of Experimental Psychology*, 17:132–138.
- 549 Rabiner, L. (1989). A tutorial on Hidden Markov Models and selected applications in speech  
550 recognition. *Proceedings of the IEEE*, 77(2):257–286.
- 551 Radvansky, G. A. and Zacks, J. M. (2017). Event boundaries in memory and cognition. *Curr Opin  
552 Behav Sci*, 17:133–140.
- 553 Ranganath, C., Cohen, M. X., Dam, C., and D’Esposito, M. (2004). Inferior temporal, prefrontal,  
554 and hippocampal contributions to visual working memory maintenance and associative memory  
555 retrieval. *Journal of Neuroscience*, 24(16):3917–3925.
- 556 Ranganath, C. and Ritchey, M. (2012). Two cortical systems for memory-guided behavior. *Nature  
557 Reviews Neuroscience*, 13:713 – 726.
- 558 Schlichting, M. L. and Preston, A. R. (2015). Memory integration: neural mechanisms and impli-  
559 cations for behavior. *Current Opinion in Behavioral Sciences*, 1:1–8.
- 560 Simony, E., Honey, C. J., Chen, J., and Hasson, U. (2016). Uncovering stimulus-locked network  
561 dynamics during narrative comprehension. *Nature Communications*, 7(12141):1–13.

- 562 Spalding, K. N., Schlichting, M. L., Zeithamova, D., Preston, A. R., Tranel, D., Duff, M. C., and  
563 Warren, D. E. (2018). Ventromedial prefrontal cortex is necessary for normal associative inference  
564 and memory integration. *The Journal of Neuroscience*, 38(15):3767–3775.
- 565 van Kesteren, M. T. R., Ruiter, D. J., Fernández, G., and Henson, R. N. (2012). How schema and  
566 novelty augment memory formation. *Trends Neurosci*, 35(4):211–9.
- 567 Waskom, M., Botvinnik, O., Okane, D., Hobson, P., David, Halchenko, Y., Lukauskas, S., Cole, J. B.,  
568 Warmenhoven, J., de Ruiter, J., Hoyer, S., Vanderplas, J., Villalba, S., Kunter, G., Quintero, E.,  
569 Martin, M., Miles, A., Meyer, K., Augspurger, T., Yarkoni, T., Bachant, P., Williams, M., Evans,  
570 Fitzgerald, C., Brian, Wehner, D., Hitz, G., Ziegler, E., Qalieh, A., and Lee, A. (2016). Seaborn:  
571 v0.7.1.
- 572 Welch, G. B. and Burnett, C. T. (1924). Is primacy a factor in association-formation. *American Journal  
573 of Psychology*, 35:396–401.
- 574 Yonelinas, A. P. (2002). The nature of recollection and familiarity: A review of 30 years of research.  
575 *Journal of Memory and Language*, 46:441–517.
- 576 Zacks, J. M., Speer, N. K., Swallow, K. M., Braver, T. S., and Reynolds, J. R. (2007). Event perception:  
577 a mind-brain perspective. *Psychological Bulletin*, 133:273–293.
- 578 Zadbood, A., Chen, J., Leong, Y. C., Norman, K. A., and Hasson, U. (2017). How we transmit  
579 memories to other brains: Constructing shared neural representations via communication. *Cereb  
580 Cortex*, 27(10):4988–5000.
- 581 Zwaan, R. A. and Radvansky, G. A. (1998). Situation models in language comprehension and  
582 memory. *Psychological Bulletin*, 123(2):162 – 185.

583 **Supporting information**

584 Supporting information is available in the online version of the paper.

585 **Acknowledgements**

586 We thank Luke Chang, Janice Chen, Chris Honey, Lucy Owen, Emily Whitaker, and Kirsten Ziman  
587 for feedback and scientific discussions. We also thank Janice Chen, Yuan Chang Leong, Kenneth  
588 Norman, and Uri Hasson for sharing the data used in our study. Our work was supported in part  
589 by NSF EPSCoR Award Number 1632738. The content is solely the responsibility of the authors  
590 and does not necessarily represent the official views of our supporting organizations.

591 **Author contributions**

592 Conceptualization: A.C.H. and J.R.M.; Methodology: A.C.H. and J.R.M.; Software: A.C.H., P.C.F.  
593 and J.R.M.; Analysis: A.C.H., P.C.F. and J.R.M.; Writing, Reviewing, and Editing: A.C.H., P.C.F.  
594 and J.R.M.; Supervision: J.R.M.

595 **Author information**

596 The authors declare no competing financial interests. Correspondence and requests for materials  
597 should be addressed to J.R.M. (jeremy.r.manning@dartmouth.edu).